TECHNICAL REPORTS

nature neuroscience

A light-gated, potassium-selective glutamate receptor for the optical inhibition of neuronal firing

Harald Janovjak[1], Stephanie Szobota[1], Claire Wyart[1], Dirk Trauner[2] & Ehud Y Isacoff[1,3]

Genetically targeted light-activated ion channels and pumps make it possible to determine the role of specific neurons in neuronal circuits, information processing and behavior. We developed a K^+-selective ionotropic glutamate receptor that reversibly inhibits neuronal activity in response to light in dissociated neurons and brain slice and also reversibly suppresses behavior in zebrafish. The receptor is a chimera of the pore region of a K^+-selective bacterial glutamate receptor and the ligand-binding domain of a light-gated mammalian kainate receptor. This hyperpolarizing light-gated channel, HyLighter, is turned on by a brief light pulse at one wavelength and turned off by a pulse at a second wavelength. The control is obtained at moderate intensity. After optical activation, the photocurrent and optical silencing of activity persists in the dark for extended periods. The low light requirement and bi-stability of HyLighter represent advantages for the dissection of neural circuitry.

Understanding the neural circuitry underlying the behavior of organisms is a fundamental challenge for both basic and clinical neuroscience. The exploration of neuronal network function has been advanced considerably through the development of new tools for the non-invasive, reversible and precise spatio-temporal manipulation of nerve cell activity using light[1,2]. Caged and photochromic neurotransmitter ligands, first invented decades ago and improved considerably since then[3], were recently joined by engineered ion channels that are controlled by covalently attached synthetic photoswitched tethered ligands (PTLs)[4,5], natural photoreceptors from vertebrates[6] and microbes[7–10], and photoswitched affinity labels that attach to and control native channels without the need for exogenous gene expression[11].

The engineered, PTL-gated ion channels and the receptors, channels and pumps of the opsin family make it possible to control neuronal excitability in specific subsets of genetically targeted cells both *in vitro* and *in vivo*. The PTL-gated ionotropic glutamate receptor 6 (iGluR6, GluK2) kainate receptor LiGluR and channelrhodopsin2 (ChR2) are cation channels that can trigger action potentials with millisecond precision[5,7]. The light-driven chloride pump Halorhodopsin (HaloR) and, more recently, proton pumps related to bacteriorhodopsin are capable of silencing neuronal activity with millisecond resolution[8–10]. Rhodopsin inhibits neurons by activating native K^+ channels via a G protein pathway, but it could have effects on other channels and signaling proteins[6]. The SPARK K^+ channel is light-blocked by a PTL[4]. Using genetic targeting, these proteins have been successfully used to control activity in select subsets of cells in embryonic chicks[6], fruit flies[12–14], *C. elegans*[15–18], zebrafish[19–22], vertebrates and mammals[23–25].

An intrinsic property of the light-driven pumps HaloR and bacteriorhodopsin is the requirement for continuous illumination. In addition, current magnitude depends on light intensity, which can result in needing intensities as high as 50 mW mm^{-2} for HaloR[26], and HaloR and bacteriorhodopsin inactivate partially under sustained illumination[8,10]. Moreover, prolonged activation of HaloR is followed by rebound excitation[19], perhaps because of efflux of the pumped Cl^-. The long-term effects of proton transport in bacteriorhodopsin have not yet been evaluated. Thus, there is a need for an alternative light-gated inhibitory system that can provide a sustained inhibitory conductance, without rebound excitation, that is triggered by low-intensity light.

We designed a K^+-selective, light-gated ion channel. To do this, we took advantage of the modular design of mammalian glutamate receptors[27–30]. iGluRs are cation channels that are permeant to Na^+ and K^+ (and in some cases to Ca^{2+}) and mediate excitatory neurotransmission in all higher organisms[31]. The iGluRs have a common, modular architecture with a prokaryotic homolog from cyanobacterium *Synechocystis* PCC 6803, sGluR0 (ref. 32), with an extracellular, bi-lobed ligand-binding domain (LBD) flanking a transmembrane ion channel (**Fig. 1**). The structures of the LBDs of several iGluRs[33,34], sGluR0 (ref. 35) and of a putative glutamate receptor from *Nostoc punctiforme*[36] were determined using X-ray crystallography and suggested that closure of the clamshell-like LBD in all of these receptors forces the opening of the transmembrane pore (**Fig. 1a**,**b**). The pore of sGluR0 is K^+ selective and its re-entrant pore loop has a GYG amino acid motif[32] typical of the K^+ channel selectivity filter. The idea that K^+ selectivity can exist in a prokaryotic glutamate receptor supports a functional resemblance and evolutionary connection of iGluRs and K^+ channels[27,29,30]. We engineered chimeric ionotropic glutamate receptors that possesses the LBD of iGluR6, including the PTL attachment site that renders it light sensitive in LiGluR[5], and combined this with the membrane-spanning domain, and thus the pore, of sGluR0. One of the chimeras functioned as a light-gated K^+ channel that responded with maximal activation at

[1]Department of Molecular and Cell Biology and Helen Wills Neuroscience Institute, University of California, Berkeley, California, USA. [2]Department of Chemistry, University of Munich, München, Germany. [3]Material Science Division and Physical Bioscience Division, Lawrence Berkeley National Laboratory, Berkeley, California, USA. Correspondence should be addressed to E.Y.I. (ehud@berkeley.edu).

Received 5 April; accepted 26 May; published online 27 June 2010; doi:10.1038/nn.2589

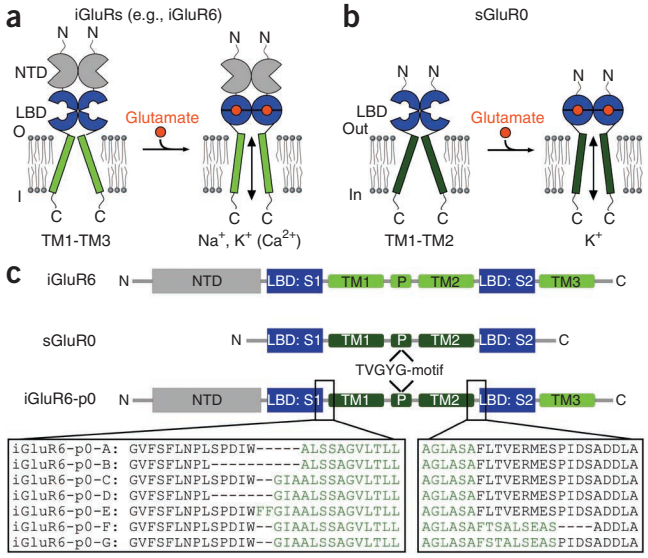

Figure 1 Chimeras of the iGluR6 LBD and the sGluR0 K^+-selective pore. (**a**) Mammalian ionotropic glutamate receptors are modular proteins with an N-terminal domain (NTD), LBD (formed by segments S1 and S2) and transmembrane ion channel (formed by transmembrane regions 1–3 (TM1–3) and the pore region (P)). Glutamate binding induces closure of the LBD and opening of a nonselective cation pore. (**b**) sGluR0 is a prokaryotic glutamate receptor that lacks an NTD and has a K^+-selective pore. (**c**) The iGluR6-p0 chimeras have the pore of sGluR0 (TM1, P with its K^+ selectivity filter signature GYG motif and TM2) inserted into iGluR6. Chimeras A–E differed at the junction between the S1 of the iGluR6 LBD and the N-terminal end of TM1 of sGluR0. Chimeras F and G used the iGluR6-p0-C S1-TM1 junction and varied in the TM2-S2 junction.

low light intensity and provides the advantageous properties of sustained photoresponses in the dark and light-induced closure.

RESULTS

sGluR0 and light-gated, K^+-selective chimeras

We first asked whether the K^+-selective sGluR0 could be converted into a tool for optical silencing of neuronal activity. We expressed a mammalian signal peptide–modified and codon-optimized version of sGluR0 in HEK293 cells. The transfected cells had small glutamate-induced currents (peak currents of 130 ± 37 pA measured at +60 mV, $n = 5$). We tested whether sGluR0 could be activated by a soluble test compound (the tether model) that has been shown to mimic the maleimide azobenzene glutamate (MAG) PTL and activate iGluR6 (ref. 5). No activation of sGluR0 was detected with 0.5–3 mM tether model (**Supplementary Fig. 1**). This lack of agonism is consistent with the observation that the ligand-binding motif of sGluR0 differs from that of the iGluRs and that the ligand docks in an opposite orientation, which would yield a steric clash with the tether[35,36]. Another problem of attempting to hyperpolarize cells with a light-gated sGluR0 is that sGluR0 activates very slowly (time constant of activation of ~290 ms[32]), too slowly for the highly temporally precise inhibition of action potential firing. Taken together, the small and slowly activating currents of sGluR0 and the lack of agonism by the MAG tether model indicated that another strategy was needed to create a light-gated inhibitory channel.

We turned to the notion of designing a K^+-selective, light-gated channel by combining the MAG photoswitching of the iGluR6 LBD[5] with the K^+ pore of sGluR0. A chimeric protein may combine the rapid activation of iGluR6 by glutamate and photoswitching[37] with the K^+ selectivity of sGluR0. AMPA and kainate receptor LBDs have already been shown to gate pores (and pore loops) of members of other iGluR families, including of the otherwise nonfunctional delta receptors[28,38]. However, although the iGluR6 LBD has been shown to gate the sGluR0 pore and the LBD of the NR1 NMDA receptor can gate several K^+ channel pore loops (not including that of sGluR0), none of these are K^+ selective[39], indicating that selectivity depends on more than just the K^+ channel pore loop. Furthermore, transplanting the GYG motif to iGluRs does not render them K^+ selective[40]. We therefore designed an alternative set of chimeras with the hope of obtaining coupling while preserving K^+ selectivity.

In the chimeric receptors, different portions of the iGluR6 pore were replaced by the corresponding codon-optimized portion of the sGluR0 pore (we refer to these as iGluR6-p0). We sought to transplant both transmembrane helices and the re-entrant pore loop of sGluR0 (TM1-P-TM2; **Fig. 1c**) while retaining the native pore-LBD

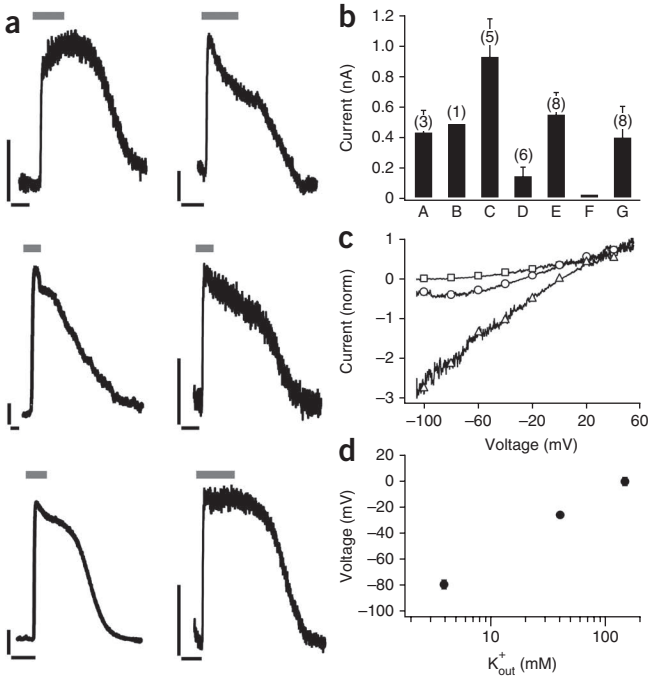

Figure 2 Glutamate gates K^+ currents in iGluR6-p0 chimeras. (**a**) Representative, glutamate-induced outward currents recorded in whole-cell mode at –20 mV after exposure to concanavalin A to block desensitization for iGluR6-p0-A (top left), iGluR6-p0-B (top right), iGluR6-p0-C (middle left), iGluR6-p0-D (middle right), iGluR6-p0-E (bottom left) and iGluR6-p0-G (bottom right). For iGluR6-p0-A, C, D, E and G, currents were observed in 60–100% of cells, whereas no currents were observed for iGluR6-p0-F and only one cell gave measurable current for iGluR6-p0-B. Black scale bars represent 100 pA and 10 s. Gray horizontal bars above traces indicate perfusion of 1.5 mM glutamate. (**b**) Average outward currents (± s.e.m.) of iGluR6-p0 chimeras induced by 1.5 mM glutamate. The largest currents were observed for iGluR6-p0-C. The numbers of observations are shown in parentheses. (**c**) Leak-subtracted current for iGluR6-p0-C with added L439C mutation for photoswitch attachment in a single HEK cell during ramp changes in membrane potential (0.16 mV ms^{-1}). Extracellular solutions contained 4 mM K^+ and 140 mM Na^+ (squares), 40 mM K^+ and 105 mM Na^+ (circles), or 145 mM K^+ and no added Na^+ (triangles). Outward rectification was consistent with voltage-dependent block of inward K^+ current by extracellular Na^+. (**d**) Reversal potentials of the glutamate-induced currents shown in **c** revealed high K^+ selectivity of iGluR6-p0-C. The s.e.m. values are the same size as the symbols ($n = 5$ at 4 and 145 mM KCl, $n = 3$ at 40 mM KCl).

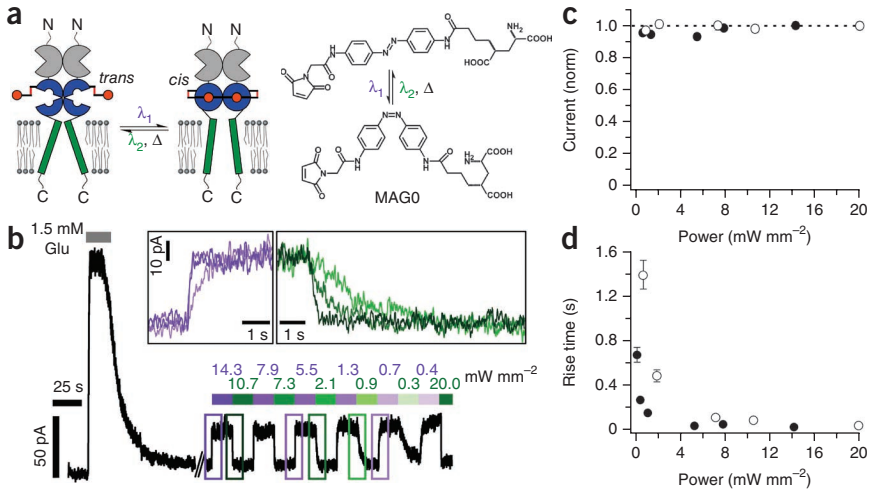

Figure 3 Photo-control of K^+ currents. (**a**) The PTL MAG0 is anchored to a cysteine residue introduced into iGluR6-p0-C (L439C). Illumination at 380 nm (violet) converts the azobenzene of MAG from *trans* to *cis* and illumination at 500 nm (green) drives the reverse isomerization, thereby conferring light sensitivity by reversibly presenting and withdrawing glutamate to and from its binding site. MAG0 consists of a glutamate, a photoisomerizable azobenzene core and a maleimide group that attaches to the cysteine. (**b**) Whole-cell currents at −20 mV in a HEK293 cell after labeling with MAG0 and concanavalin A. Reversible photocurrents are 17.7% the size of glutamate-evoked currents. Insets, photocurrent activation and deactivation at high, medium and low light intensities. (**c**) Steady-state current amplitude was saturated above 1 mW mm^{-2}. Receptor activation by ultraviolet light (filled symbols) and deactivation by green light (open symbols) were normalized to currents at highest power. (**d**) Reducing light intensity below 5 mW mm^{-2} slowed the rate of current activation by light.

linkers of iGluR6. In the absence of crystal structures, we estimated the locations of the ends of the helices in sGluR0 and iGluR6 using sequence comparison to two K^+ channels with known structures, KcsA and Kv1.2, and hydropathy analysis (**Supplementary Fig. 2**). Several excision sites were chosen and a total of seven unique chimeras were generated and tested.

Our first set of chimeras, iGluR6-p0-A, B, C, D and E, varied only in the most N-terminal residues of the transplanted pore (**Fig. 1c**). When functionally testing chimeras in HEK293 cells, we recorded large, stable glutamate-induced outward currents at −20 mV for iGluR6-p0-A, C, D and E (**Fig. 2a**). Because iGluR6-p0-C gave particularly large outward currents (941 ± 239 pA, $n = 8$; **Fig. 2a**,**b**), we focused on this variant for further modifications. The iGluR6-p0-C chimera was refined into two additional variant chimeras, iGluR6-p0-F and G, in which residues in the C-terminal pore-LBD linker were replaced with residues from sGluR0. No glutamate-induced responses were detected for iGluR6-p0-F and the currents of iGluR6-p0-G (303 ± 130 pA, $n = 8$) were substantially smaller than those of iGluR6-p0-C (**Fig. 2a**,**b**). The latter observation agrees with a previously proposed functional interaction of residues in this linker and the LBD in iGluR6 (ref. 41).

Photoswitching iGluR6-p0

Having found that iGluR6-p0-C had the largest glutamate-induced currents of the iGluR6-p0 chimeras, we combined it with the MAG attachment site of the best photoswitching version of LiGluR, a leucine to cysteine substitution at position 439 (ref. 42). HEK293 cells expressing iGluR6-p0-C-L439C had a mean glutamate-induced current of 745 ± 252 pA. This final construct, termed HyLighter, had reversal potentials of glutamate-induced currents of −79.7 ± 3.0, −26.5 ± 0.0 and −1.0 ± 2.7 mV when the external K^+ concentration was adjusted to 4, 40 and 145 mM KCl, respectively (**Fig. 2c**,**d**). Analysis of these reversal potentials with the Goldman-Hodgkin-Katz equation indicates a K^+:Na^+ permeability ratio of ~100:1. Current-voltage traces (**Fig. 2c**) exhibited the same kind of outward rectification in the presence of extracellular Na^+ that was seen previously in sGluR0 and attributed to Na^+ block of inward K^+ current[32], indicating that the sGluR0 pore maintains its character when controlled by the iGluR6 LBD in iGluR6-p0-C.

We tested the ability of HyLighter to be photo-controlled by MAG0, the shortest MAG PTL (Online Methods; **Fig. 3a**). After labeling with 40–60 μM MAG0 for 20 min, we measured glutamate-induced currents in the dark, followed by alternating illumination at 380 nm to drive isomerization of MAG0 to the *cis*-state and 500 nm to drive isomerization to the *trans*-state. The photocurrents were 15.2 ± 4.0% ($n = 4$) of the size of the glutamate-evoked currents. Maximal photocurrents were reached at modest light intensities (**Fig. 3b**,**c**). For example, illumination with 380 nm at 0.7 mW mm^{-2} resulted in 95.8 ± 1.9% of current achieved with maximal light intensity (14.3 mW mm^{-2}), whereas illumination with 500 nm at 0.9 mW mm^{-2} resulted in 97.3 ± 1.0% of the current seen at 20.0 mW mm^{-2} ($n = 4$). The time course of the photocurrents was intensity dependent. At maximal light intensity, half-maximal photocurrents were reached in 28.5 ± 2.8 ms at 380 nm and half-maximal deactivation was reached in 42.1 ± 1.7 ms at 500 nm ($n = 4$; **Fig. 3d**). The slower off-speed could be a result of a stabilization of MAG0 in the *cis*-state by the binding of its glutamate end to the LBD binding pocket. Such stabilization could also slow thermal *cis* to *trans* isomerization when the glutamate end of MAG is bound in the receptor. Indeed, we detected no change in current over tens of minutes in LiGluR[37]. Using kinetic modeling (Online Methods) and taking into account the fact that unbound *cis*-MAG1 has a lifetime of ~25 min[37], we found that a stabilization of a few kJ mol^{-1}, equivalent to the energy of a hydrogen bond, was sufficient to increase *cis*-state lifetime by one order of magnitude. This prolonged activated state in the dark combined with the ability to rapidly turn HyLighter off is a unique feature among proteins capable of hyperpolarizing cells with light (see below).

Optical suppression of neuronal firing and behavior

In cultured hippocampal neurons expressing HyLighter under the control of the CMV promoter, brief light pulses at 380 nm triggered photocurrents with a mean amplitude of 92.8 ± 13.2 pA in whole-cell voltage-clamp mode (at a holding potential of −45 mV, $n = 3$; **Fig. 4a**). In whole-cell current-clamp mode, the same light pulse evoked hyperpolarizations of 10.2 ± 3.1 mV (**Fig. 4a**). Addition of the endoplasmatic reticulum–forward trafficking motif of Kir2.1[43], in combination with the *SYN1* promoter, increased currents to 225 ± 28 pA and hyperpolarizations to 15.8 ± 2.0 mV. Once the photocurrent or photo-hyperpolarization was triggered by the 380-nm light pulse, it remained constant in the dark until deactivation was induced by a light pulse at 500 nm (**Fig. 4a**). Photocurrents could be repeatedly activated and deactivated for hundreds of cycles without deterioration (**Supplementary Fig. 3**).

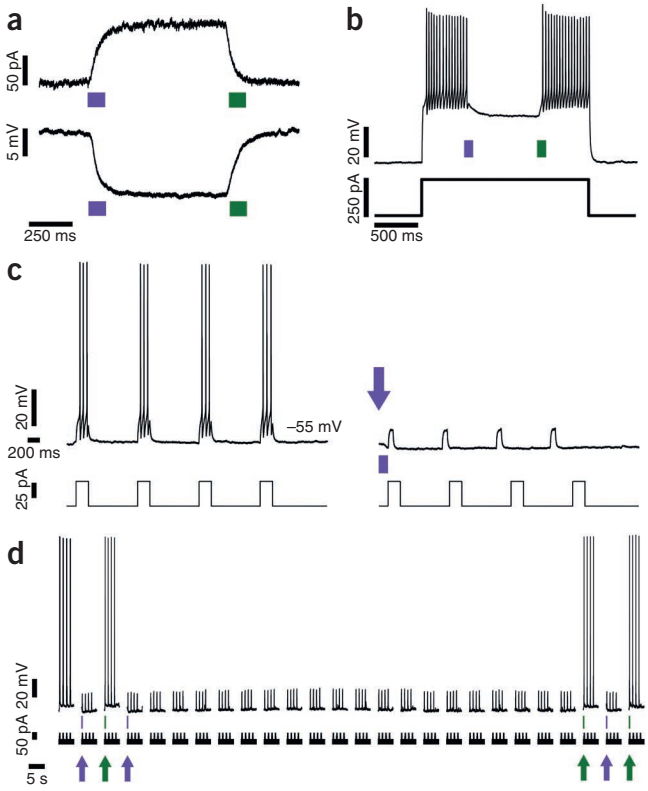

Figure 4 Optical inhibition of neuronal activity in dissociated cultured hippocampal neurons. (**a**) Photocurrent measured in whole-cell voltage clamp (top) and photo-hyperpolarization measured in whole-cell current clamp (bottom) recorded at –45-mV membrane potential in a hippocampal neuron expressing HyLighter, following labeling with MAG. Brief (100 ms) pulses of 380-nm light (violet bars) activated the channels, which remained open in the dark and were then deactivated by 500-nm light (green bars). (**b**) Action potential firing evoked by a 250-pA pulse was silenced by 380-nm light (violet bar). The silencing persisted until Hylighter was turned off by 500-nm light (green bar). (**c**) Action potential firing evoked by a four-pulse train of 50-pA depolarizing current injections was silenced by a single light pulse. Arrow indicates brief (350 ms) illumination at 380 nm. (**d**) Inhibition of action potential firing after a single 380-nm light (violet arrows) pulse persisted for seconds to minutes, until HyLighter is switched off by a pulse of 500-nm light (green arrows). Four-pulse depolarizing current trains were given once every 7.75 s. Note that different neurons are depicted in **c** and **d**.

Action potentials triggered by the somatic injection of current through the recording pipette were suppressed by activation of HyLighter. Firing was suppressed throughout a long depolarization that triggered a train of action potentials (**Fig. 4b**) and in response to short bursts of action potentials during short depolarizations induced by repeated pulses of current injection (**Fig. 4c**). The hyperpolarization and suppression of firing persisted without decrement for extended periods (minutes) in the dark until HyLighter was rapidly turned off with a pulse of 500-nm light (**Fig. 4d**). HyLighter did not appear to alter the properties of the neurons in which it was expressed. HyLighter-expressing cells and nontransfected cells in the same preparation had similar resting potentials (–59.9 ± 4.4 mV and –54.3 ± 1.8 mV, respectively) and action potential frequencies (40.7 ± 6.6 Hz and 37.3 ± 1.8 Hz, respectively; $n = 3$) in response to long steps of depolarizing current injection.

Extending the technique to intact brain preparations, we examined HyLighter in cultured hippocampal slices. Slices were prepared from the hippocampi of early postnatal rats, cultured at 34 °C and transfected with HyLighter-GFP by Biolistic gene transfer. HyLighter was expressed equally well in all regions of the hippocampus (data not shown) and the HyLighter-GFP protein was found to be homogeneously distributed throughout all parts of the neuron (**Supplementary Fig. 4**). After a brief incubation with MAG0, whole-cell recordings from individual neurons in the slice revealed that activation of HyLighter by illumination at 390 nm induced membrane hyperpolarization, and, when this took place during a train of action potentials that were evoked by depolarizing current injection, the HyLighter induced hyperpolarization robustly silenced firing (**Fig. 5**). The hyperpolarization induced by activation of HyLighter was strong and was sustained until HyLighter was deactivated by 500-nm light.

To test HyLighter function *in vivo*, we generated transgenic zebrafish expressing HyLighter and examined the effect of light on behavior. Fish expressing HyLighter-GFP under the control of a UAS promoter were crossed to fish from an enhancer trap line in which the GAL4 transcription factor is expressed in spinal cord motor neurons (line *Gal4*^{s1020t}; **Fig. 6a**)[22,44]. Escape responses were triggered by a mechanical stimulus to the dish and we monitored behavior by observing the motions of the free tail in head-embedded fish larvae. The fish were first labeled with the MAG photoswitch at 5 d post fertilization, as previously described[21,22]. Bouts of mechanical stimulation were administered in the absence of illumination, following illumination of the tail with 390-nm light (0.5 mW mm^{-2}) to activate HyLighter and following illumination at 500 nm (0.5 mW mm^{-2}) to deactivate HyLighter. Illumination at 390 nm reduced the probability of an escape response ($P < 0.01$, $n = 14$; **Fig. 6b**) and this effect was reversed by illumination at 500 nm. The same illumination had no effect on the probability of escape responses in siblings from the same crosses that did not express HyLighter ($P > 0.31$, $n = 16$).

DISCUSSION

Light-controlled systems provide many advantages for artificially manipulating biological function *in vivo* with high spatial and temporal resolution and precise control of signal strength. Proteins that bind natural or synthetic photoswitches have made it possible to probe neuronal networks[1,2] by asking how turning on and off the activity of specific cells alters information processing and behavior. Although a number of light-controlled, genetically targetable excitatory systems

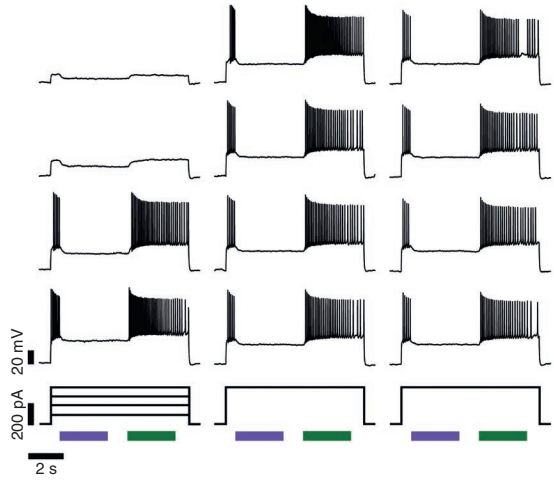

Figure 5 Silencing of activity in cultured hippocampal slice. Action potentials triggered by current injections (up to 400 pA) are reliably silenced by activation of HyLighter at 390 nm (violet bar) and released from inhibition by deactivation of HyLighter at 500 nm (green bar).

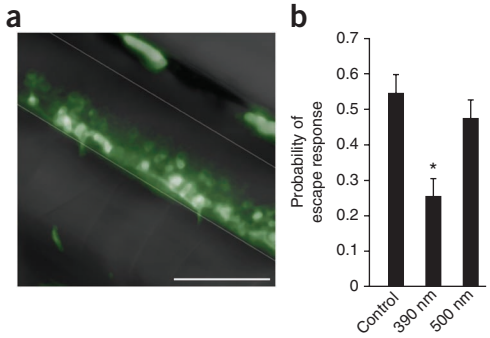

Figure 6 HyLighter expressed in motorneurons of zebrafish larvae reversibly suppresses escape response. (**a**) Expression of HyLighter-GFP (UAS: iGluR-p0-C-L439C-GFP) in the *Gal4*^{s1020t} driver line, which targets motorneurons in the ventral half of the spinal cord. Ventral (lower left) and dorsal (upper right) limits of the spinal cord are indicated by gray lines. Rostral is on the left, caudal on the right. Scale bar represents 50 µm. (**b**) Compared to the initial no illumination (control), the probability of response to a mechanical stimulus (tap on the dish) was suppressed by activation of HyLighter with illumination at 390 nm of neurons in the tail before the stimulus (*$P < 0.01$, $n = 14$). The escape response recovered after illumination at 500 nm (which deactivates HyLighter) to a level no different from the initial control ($P > 0.57$, $n = 14$). Error bars are s.e.m.

have been developed[5,7,45], the only light-activated inhibitory proteins offering millisecond-resolution are pumps of the bacteriorhodopsin and HaloR families[8–10].

We rationally designed a ligand-gated ion channel that is both K^+ selective and light controlled with properties and advantages that are distinct from those of SPARK, HaloR and bacteriorhodopsins. Chimeras were constructed in which the transmembrane helices and re-entrant pore loop of the K^+-selective sGluR0 were transplanted into iGluR6; the best of these was modified for light gating and termed HyLighter. HyLighter is light activated and is therefore not active before photoswitch conjugation. This is an advantage over light-blocked SPARK, one that minimizes the risk of compensatory changes before photoswitch conjugation. HyLighter is more sensitive to light than HaloR, reaching maximal current over a wide range of intensities to achieve substantial steady-state inhibition. HyLighter also has the unique property of converting a pulse of light into a stable hyperpolarizing current, which remains on for extended periods in the dark and can then be turned off at will by the complementary wavelength of light. This property could be valuable for behavioral experiments, where incidental visual stimulation may be a confound.

HyLighter requires a synthetic photoswitch, MAG, which must be delivered into the expressing tissue. MAG has been shown to successfully reach deep neural tissue in zebrafish; MAG was simply added to the water to conjugate to the iGluR6 receptor clamshell and generate the excitatory light-gated LiGluR channel[21], permitting an analysis of the neural basis of behavior[22]. MAG diffusion into the zebrafish was also efficient enough to endow HyLighter with light sensitivity and thereby impart the opposite light-gated inhibition. Moreover, we found that MAG also penetrated mammalian brain slices well enough to permit as intense a light-gated inhibition as seen in dissociated neurons. As optogenetic studies in the mammalian brain require light delivery through implanted light sources, it may be possible to deliver MAG through the same portal that is used to place a fiber optic or a lens. Indeed, the delivery of the photoswitch under illumination could be used to pattern photo-affinity labeling[37] to restrict receptor functionalization spatially.

As was recently done with the chimeric redesign of rhodopsin to control new G protein signaling cascades[46], HyLighter borrows the light gating of one protein and staples it onto the functional domain of another to obtain a light-gated functionality. HyLighter complements the existing optogenetic tools as a new, light-activated, purely hyperpolarizing ion channel. Its distinct push-pull two-wavelength design, low light requirement and unique spectral sensitivity expand possible applications for suppressing activity in specific cells in intact neural circuits while providing temporal precision. Bi-stability allows experiments in which cells can be silenced by light and behavioral analysis can be carried out afterwards in ambient light or in the dark in the absence of a possible visual confound.

METHODS

Methods and any associated references are available in the online version of the paper at http://www.nature.com/natureneuroscience/.

Note: Supplementary information is available on the Nature Neuroscience website.

ACKNOWLEDGMENTS

We thank K. Partin, K. Kainanen, E. Gouaux and M. Hollmann for constructs, G. Sandoz, P. Koprowski and F. Tombola for discussions, D. Fortin, T. Tracey, K. Greenberg, A. Pham, M. Soden, H. Lu, E. Warp, K. McDaniel, R. Arant and Z. Fu for technical assistance, and M. Volgraf and V. Franckevicius for MAG compounds. This work was supported by the US National Institutes of Health Nanomedicine Development Center for the Optical Control of Biological Function (5PN2EY018241), the Human Frontier Science Program (RPG23-2005), the National Science Foundation (FIBR 43C-1081892), a fellowship of the European Molecular Biology Organization (to H.J.) and a Marie-Curie fellowship (to C.W.; the fellowship was obtained with the laboratory CNRS-UMR5020 'Neurosciences Sensorielles, Comportement Cognition').

AUTHOR CONTRIBUTIONS

H.J. designed chimeric proteins, conducted experiments in HEK293 cells and neuronal cultures, contributed to experiments in brain slices and zebrafish, analyzed data and wrote the manuscript. S.S. conducted experiments in brain slices, analyzed data and wrote the manuscript. C.W. conducted experiments in zebrafish, analyzed data and wrote the manuscript. D.T. developed photoswitching methodology and provided photoswitches. E.Y.I. designed chimeric proteins, developed photoswitching methodology, analyzed data and wrote the manuscript.

COMPETING FINANCIAL INTERESTS

The authors declare no competing financial interests.

Published online at http://www.nature.com/natureneuroscience/.
Reprints and permissions information is available online at http://www.nature.com/reprintsandpermissions/.

1. Herlitze, S. & Landmesser, L.T. New optical tools for controlling neuronal activity. *Curr. Opin. Neurobiol.* **17**, 87–94 (2007).
2. Zhang, F., Aravanis, A.M., Adamantidis, A., de Lecea, L. & Deisseroth, K. Circuit-breakers: optical technologies for probing neural signals and systems. *Nat. Rev. Neurosci.* **8**, 577–581 (2007).
3. Ellis-Davies, G.C. Caged compounds: photorelease technology for control of cellular chemistry and physiology. *Nat. Methods* **4**, 619–628 (2007).
4. Banghart, M., Borges, K., Isacoff, E., Trauner, D. & Kramer, R.H. Light-activated ion channels for remote control of neuronal firing. *Nat. Neurosci.* **7**, 1381–1386 (2004).
5. Volgraf, M. *et al.* Allosteric control of an ionotropic glutamate receptor with an optical switch. *Nat. Chem. Biol.* **2**, 47–52 (2006).
6. Li, X. *et al.* Fast noninvasive activation and inhibition of neural and network activity by vertebrate rhodopsin and green algae channelrhodopsin. *Proc. Natl. Acad. Sci. USA* **102**, 17816–17821 (2005).
7. Boyden, E.S., Zhang, F., Bamberg, E., Nagel, G. & Deisseroth, K. Millisecond-timescale, genetically targeted optical control of neural activity. *Nat. Neurosci.* **8**, 1263–1268 (2005).
8. Chow, B.Y. *et al.* High-performance genetically targetable optical neural silencing by light-driven proton pumps. *Nature* **463**, 98–102 (2010).
9. Han, X. & Boyden, E.S. Multiple-color optical activation, silencing, and desynchronization of neural activity, with single-spike temporal resolution. *PLoS One* **2**, e299 (2007).
10. Zhang, F. *et al.* Multimodal fast optical interrogation of neural circuitry. *Nature* **446**, 633–639 (2007).
11. Fortin, D.L. *et al.* Photochemical control of endogenous ion channels and cellular excitability. *Nat. Methods* **5**, 331–338 (2008).

12. Suh, G.S.B. *et al.* Light activation of an innate olfactory avoidance response in *Drosophila*. *Curr. Biol.* **17**, 905–908 (2007).
13. Zhang, W., Ge, W.P. & Wang, Z.R. A toolbox for light control of *Drosophila* behaviors through Channelrhodopsin 2–mediated photoactivation of targeted neurons. *Eur. J. Neurosci.* **26**, 2405–2416 (2007).
14. Schroll, C. *et al.* Light-induced activation of distinct modulatory neurons triggers appetitive or aversive learning in *Drosophila* larvae. *Curr. Biol.* **16**, 1741–1747 (2006).
15. Franks, C.J., Murray, C., Ogden, D., O'Connor, V. & Holden-Dye, L. A comparison of electrically evoked and channel rhodopsin–evoked postsynaptic potentials in the pharyngeal system of *Caenorhabditis elegans*. *Invert. Neurosci.* **9**, 43–56 (2009).
16. Liu, Q., Hollopeter, G. & Jorgensen, E.M. Graded synaptic transmission at the *Caenorhabditis elegans* neuromuscular junction. *Proc. Natl. Acad. Sci. USA* **106**, 10823–10828 (2009).
17. Liewald, J.F. *et al.* Optogenetic analysis of synaptic function. *Nat. Methods* **5**, 895–902 (2008).
18. Nagel, G. *et al.* Light activation of channelrhodopsin-2 in excitable cells of *Caenorhabditis elegans* triggers rapid behavioral responses. *Curr. Biol.* **15**, 2279–2284 (2005).
19. Arrenberg, A.B., Del Bene, F. & Baier, H. Optical control of zebrafish behavior with halorhodopsin. *Proc. Natl. Acad. Sci. USA* **106**, 17968–17973 (2009).
20. Douglass, A.D., Kraves, S., Deisseroth, K., Schier, A.F. & Engert, F. Escape behavior elicited by single, channelrhodopsin-2–evoked spikes in zebrafish somatosensory neurons. *Curr. Biol.* **18**, 1133–1137 (2008).
21. Szobota, S. *et al.* Remote control of neuronal activity with a light-gated glutamate receptor. *Neuron* **54**, 535–545 (2007).
22. Wyart, C. *et al.* Optogenetic dissection of a behavioral module in the vertebrate spinal cord. *Nature* **461**, 407–410 (2009).
23. Ayling, O.G.S., Harrison, T.C., Boyd, J.D., Goroshkov, A. & Murphy, T.H. Automated light-based mapping of motor cortex by photoactivation of channelrhodopsin-2 transgenic mice. *Nat. Methods* **6**, 219–224 (2009).
24. Lagali, P.S. *et al.* Light-activated channels targeted to ON bipolar cells restore visual function in retinal degeneration. *Nat. Neurosci.* **11**, 667–675 (2008).
25. Gradinaru, V., Mogri, M., Thompson, K.R., Henderson, J.M. & Deisseroth, K. Optical deconstruction of Parkinsonian neural circuitry. *Science* **324**, 354–359 (2009).
26. Zhao, S. *et al.* Improved expression of halorhodopsin for light-induced silencing of neuronal activity. *Brain Cell Biol.* **36**, 141–154 (2008).
27. Kuner, T., Seeburg, P.H. & Guy, H.R. A common architecture for K^+ channels and ionotropic glutamate receptors? *Trends Neurosci.* **26**, 27–32 (2003).
28. Villmann, C., Strutz, N., Morth, T. & Hollmann, M. Investigation by ion channel domain transplantation of rat glutamate receptor subunits, orphan receptors and a putative NMDA receptor subunit. *Eur. J. Neurosci.* **11**, 1765–1778 (1999).
29. Wo, Z.G. & Oswald, R.E. Unraveling the modular design of glutamate-gated ion channels. *Trends Neurosci.* **18**, 161–168 (1995).
30. Wood, M.W., VanDongen, H.M. & VanDongen, A.M. Structural conservation of ion conduction pathways in K channels and glutamate receptors. *Proc. Natl. Acad. Sci. USA* **92**, 4882–4886 (1995).
31. Gereau, R.W. IV & Swanson, G. *The Glutamate Receptors, Vol. 1* (Humana Press, Totowa, New Jersey, 2008).
32. Chen, G.Q., Cui, C., Mayer, M.L. & Gouaux, E. Functional characterization of a potassium-selective prokaryotic glutamate receptor. *Nature* **402**, 817–821 (1999).
33. Hansen, K.B., Yuan, H. & Traynelis, S.F. Structural aspects of AMPA receptor activation, desensitization and deactivation. *Curr. Opin. Neurobiol.* **17**, 281–288 (2007).
34. Mayer, M.L. Glutamate receptor ion channels. *Curr. Opin. Neurobiol.* **15**, 282–288 (2005).
35. Mayer, M.L., Olson, R. & Gouaux, E. Mechanisms for ligand binding to GluR0 ion channels: crystal structures of the glutamate and serine complexes and a closed apo state. *J. Mol. Biol.* **311**, 815–836 (2001).
36. Lee, J.H. *et al.* Crystal structure of the GluR0 ligand-binding core from *Nostoc punctiforme* in complex with L-glutamate: structural dissection of the ligand interaction and subunit interface. *J. Mol. Biol.* **376**, 308–316 (2008).
37. Gorostiza, P. *et al.* Mechanisms of photoswitch conjugation and light activation of an ionotropic glutamate receptor. *Proc. Natl. Acad. Sci. USA* **104**, 10865–10870 (2007).
38. Schmid, S.M., Kott, S., Sager, C., Huelsken, T. & Hollmann, M. The glutamate receptor subunit delta2 is capable of gating its intrinsic ion channel as revealed by ligand binding domain transplantation. *Proc. Natl. Acad. Sci. USA* **106**, 10320–10325 (2009).
39. Hoffmann, J., Villmann, C., Werner, M. & Hollmann, M. Investigation via ion pore transplantation of the putative relationship between glutamate receptors and K^+ channels. *Mol. Cell. Neurosci.* **33**, 358–370 (2006).
40. Hoffmann, J., Gorodetskaia, A. & Hollmann, M. Ion pore properties of ionotropic glutamate receptors are modulated by a transplanted potassium channel selectivity filter. *Mol. Cell. Neurosci.* **33**, 335–343 (2006).
41. Yelshansky, M.V., Sobolevsky, A.I., Jatzke, C. & Wollmuth, L.P. Block of AMPA receptor desensitization by a point mutation outside the ligand-binding domain. *J. Neurosci.* **24**, 4728–4736 (2004).
42. Numano, R. *et al.* Nanosculpting reversed wavelength sensitivity into a photoswitchable iGluR. *Proc. Natl. Acad. Sci. USA* **106**, 6814–6819 (2009).
43. Ma, D. *et al.* Role of ER export signals in controlling surface potassium channel numbers. *Science* **291**, 316–319 (2001).
44. Scott, E.K. *et al.* Targeting neural circuitry in zebrafish using GAL4 enhancer trapping. *Nat. Methods* **4**, 323–326 (2007).
45. Zemelman, B.V., Lee, G.A., Ng, M. & Miesenbock, G. Selective photostimulation of genetically chARGed neurons. *Neuron* **33**, 15–22 (2002).
46. Airan, R.D., Thompson, K.R., Fenno, L.E., Bernstein, H. & Deisseroth, K. Temporally precise *in vivo* control of intracellular signaling. *Nature* **458**, 1025–1029 (2009).

ONLINE METHODS

Synthesis of MAG photoswitches. MAG0, MAG1 and tether model synthesis and chemical analysis were described previously[5,42].

Protein construction and site-directed mutagenesis. A DNA segment coding for the sGluR0 pore was synthesized with mammalian codon optimization according to the supplier's recommendation (Epoch Biolabs). The a-splice isoform of iGluR6 was obtained from K. Partin (Colorado State University). An initial iGluR6-p0-variant was created by cloning the sGluR0 pore into iGluR6 using introduced sites for Bsp68I and BstEII restriction enzymes (New England Biolabs). To generate iGluR6-p0-A to G, regions flanking the sGluR0 pore were extended by PCR and 5′-phosphorylated oligonucleotides with corresponding overhangs. For testing, residues 32 to the last residue of iGluR6-p0-A to G were subcloned into pcDNA3.1 containing a viral signal peptide (K. Kainanen, University of Helsinki)[47]. eGFP-tagged iGluR-p0-C-L439C was obtained by introducing the L439C substitution and subcloning into the pEGFP-N1 vector containing the native iGluR6 signal peptide and a WPR element for optimized expression. iGluR-p0-C-L439C-GFP-WPRE was then subcloned into pcDNA3.1 containing the human *SYN1* promoter. Restrictions sites and point substitutions were introduced by site-directed mutagenesis (Quickchange XL, Stratagene). Residues are numbered according to the start methionine of wild-type iGluR6. Codon-optimized sGluR0 cDNA with a modified signal peptide was obtained from E. Gouaux (Oregon Health and Science University)[32].

HEK293 and neuron culture and transfection. HEK293 cells were maintained in DMEM (Invitrogen) with 5% fetal bovine serum (vol/vol, Sigma), seeded on glass coverslips coated with poly-lysine (Sigma) and transfected with glutamate receptors and eYFP in pEGFP-N1 at a ratio of 20:1 with Lipofectamine 2000 (Invitrogen). Dissociated postnatal rat hippocampal neurons (postnatal days 0–5) were prepared and transfected using calcium phosphate as described previously[21].

MAG conjugation to HEK293 cells and neurons. To conjugate MAG0 in HEK293 cells, we diluted MAG0 to 40–60 μM in extracellular recording solution containing 145 mM NaCl, 4 mM KCl, 1 mM $MgCl_2$, 2 mM $CaCl_2$ and 10 mM HEPES (pH 7.4). After illumination of MAG with 380-nm light (0.19 mW mm^{-2}) for 2 min, cells were incubated for 20–25 min at 20–25 °C in the dark and then rinsed with extracellular recording solution. Prior to recording, the HEK293 cells were incubated in an extracellular solution containing 0.3 mg ml^{-1} concanavalin A type VI (Sigma) to block desensitization of iGluR6. Concanavalin was applied only to HEK293 cells and never to neurons. For neurons, MAG was diluted in a solution containing 150 mM NMDG-HCl, 3 mM KCl, 0.5 mM $CaCl_2$, 5 mM $MgCl_2$, 10 mM HEPES and 5 mM glucose (pH 7.4). After illumination of MAG with 380-nm light for 2 min, cells were incubated for 20–25 min at 20–25 °C in the dark and then rinsed with extracellular recording solution.

Electrophysiology and light switching in cultured cells. Whole-cell patch-clamp recordings were performed with an Axopatch 200A amplifier (Molecular Devices) 36–72 h after transfection for HEK cells and 2–5 d after transfection for neurons. Pipettes had resistances of 3–5 MΩ and were filled with a solution containing 140 mM KCl, 5 mM EGTA, 0.5 mM $CaCl_2$, 1.0 mM $MgCl_2$ and 10 mM HEPES (pH 7.4) for HEK cells or 135 mM potassium gluconate, 10 mM NaCl, 10 mM HEPES, 2 mM $MgCl_2$, 2 mM MgATP and 1 mM EGTA (pH 7.4) for neurons. For HEK cell recordings, perfusion with extracellular solution (see above) was continuous, with 1.5 mM glutamate added as indicated. For reversal potential measurements, extracellular Na^+ was replaced by K^+. For neuron recordings, 25 μM 6,7-dinitroquinoxaline-2,3-dione and 10 mM glucose was added to the extracellular solution. Illumination was applied using a 300-W wavelength-switching system with 1–2-ms switching time (DG-4P, Sutter Instruments) connected to the back illumination port of the microscope (IX70, Olympus). Light intensities were determined using a power meter (Newport). Filters for 380- and 500-nm illumination (Semrock) had bandwidths of 34 and 25 nm, respectively, and were directed to a 20× objective (Olympus) using a total reflectance mirror (Edmund Optics). Electrophysiological data was recorded with pClamp software (Molecular Devices), which was also used to automatically control the illumination device. Only neurons with a resting potential ≤−50 mV were analyzed.

Preparation of cultured hippocampal slices. Hippocampi were obtained from postnatal Sprague-Dawley rats (postnatal days 6 and 7), cut into 400-μm slices and cultured on 0.4-μm Millicell culture inserts (Millipore) in Neurobasal-A medium (Gibco) supplemented with 20% horse serum (vol/vol), insulin, ascorbic acid, GlutaMAX (Gibco), penicillin/streptomycin, HEPES and Ara-C. Slices were transfected 1 d after isolation by Biolistic gene transfer using a BioRad Helios Gene Gun and gold microcarriers coated with both Hylighter-GFP-WPRE (in pcDNA3.1 containing human *SYN1*) and cytosolic tdTomato DNA (to aid in the visualization of the transfected cells).

MAG conjugation and hippocampal slice electrophysiology. Electrophysiological recordings were obtained from slices after 6–9 d *in vitro*. Just before recording, slices were incubated at 20–25 °C for 30 min with MAG0 (250 μM) diluted in NMDG-labeling solution (150 mM NMDG-HCl, 3 mM KCl, 0.5 mM $CaCl_2$, 5 mM $MgCl_2$, 10 mM HEPES and 5 mM glucose, pH 7.4). Slices were rinsed twice in labeling solution before recording. Whole-cell patch-clamp recordings were performed on an upright Zeiss AxioExaminer using an Axopatch 200B amplifier (Molecular Devices). Pipettes had resistances of 3–5 MΩ and were filled with the neuron pipette solution containing (135 mM potassium-gluconate, 10 mM NaCl, 10 mM HEPES, 2 mM $MgCl_2$, 2 mM MgATP and 1 mM EGTA, pH 7.4). The slices were perfused with aCSF consisting of 119 mM NaCl, 2.5 mM KCl, 1.3 mM $MgSO_4$, 1 mM NaH_2PO_4-H_2O, 26.2 mM $NaHCO_3$, 11 mM glucose and 2.5 mM $CaCl_2$. The aCSF was continually circulated and bubbled with 95% O_2/5% CO_2. The light used for photoswitching was from a DG-4 (Sutter Instruments) coupled to the microscope and projected onto the sample through a digital micromirror device (Mosaic System, Photonic Instruments) through a 40× objective. Light intensity at the sample was approximately 20 mW mm^{-2} at 390 nm and 40 mW mm^{-2} at 500 nm. In many cases, the illumination area was smaller than the neuron and distal processes were not subject to photostimulation.

Generation of stable zebrafish transgenic line. To make the *UAS: iGluR-p0-C-L439C-GFP* transgenic construct, *iGluR-p0-C-L439C-GFP* was subcloned in between the Tol2 recognition sequences in the pT2KXIGΔin vector[48]. *Gal4*^{s1020t} embryos[22,44] were injected at the one-cell stage with a solution of 25 ng μl^{-1} *UAS: iGluR-p0-C-L439C-GFP* DNA, 50 ng μl^{-1} transposase mRNA and 0.04% Phenol Red (vol/vol). F1 embryos were screened by fluorescence and used for experiments 5 d post fertilization.

MAG labeling and photostimulation on zebrafish larvae. MAG1 and MAG0 were diluted to 5 mM in DMSO and pre-activated by ultraviolet light (365 nm) for 5 min. The E3 medium was then added to reach a final concentration of 100 μM MAG. We bathed 5-d-old larvae in the labeling solution for 30 min at 28.5 °C. The larvae were then washed three times with fresh E3 medium. Following a 1-h recovery period, all spontaneously swimming larvae were embedded in agar and their tails were freed. The light source used for photoswitching was a DG-4 (Sutter Instruments) coupled to an upright Zeiss AxioExaminer epifluorescence microscope (the light power was 0.5 mW mm^{-2} at 390 nm and 500 nm). Escape responses were induced by mechanical taps to the dish at a 10-s interstimulus interval. Ultraviolet light pulses (1–5-second duration) illuminating the tail were immediately followed by the mechanical stimulus. Motion of the tail was monitored under low-light conditions at 60 frames per s using a CCD camera coupled to the side port of the AxioExaminer microscope and a 5× objective. The tracking of the tail position was performed using a custom-made script written in Matlab 2007 (Mathworks).

Kinetic model. We describe MAG with a two-state model in which the high energy *cis*-state is separated from the low-energy *trans*-state by a single energy barrier. In the dark after ultraviolet illumination, the only existing reaction is the thermally activated *cis-trans* isomerization. This process can be described by an Arrhenius-type equation[49,50], $\frac{1}{\tau} = Ae^{-\frac{E_A}{k_B T}}$, where τ denotes *cis*-state lifetime, A denotes attempt frequency (≈10^{10} s^{-1} for azobenzenes[49,50]), E_A denotes activation energy (that is, height of the energy barrier) and $k_B T$ denotes thermal energy. E_A can be determined to be ≈75 kJ mol^{-1} by inserting a τ of 25.47 min[37] into the Arrhenius equation after rearranging. This value agrees well with that of other

azobenzene photoswitches[49,50]. Finally, the Arrhenius equation allows estimating that increasing E_A by less than 10% (6 kJ mol^{-1}) will result in an increased lifetime of one order of magnitude.

47. Pasternack, A. *et al.* Alpha-amino-3-hydroxy-5-methyl-4-isoxazolepropionic acid (AMPA) receptor channels lacking the N-terminal domain. *J. Biol. Chem.* **277**, 49662–49667 (2002).
48. Kotani, T., Nagayoshi, S., Urasaki, A. & Kawakami, K. Transposon-mediated gene trapping in zebrafish. *Methods* **39**, 199–206 (2006).
49. Borisenko, V. & Woolley, G.A. Reversibility of conformational switching in light-sensitive peptides. *J. Photochem. Photobiol. A Chem.* **173**, 21–28 (2005).
50. Bunce, N.J., Ferguson, G., Forber, C.L. & Stachnyk, G.J. Sterically hindered azobenzenes: isolation of cis isomers and kinetics of thermal cis > trans isomerization. *J. Org. Chem.* **52**, 394–398 (1987).

doi:10.1038/nn.2589